Upregulation of gluconeogenesis leads to increased tolerance to antibiotics targeting the MreB elongosome in *E. coli*

Brody Barton, Addison Grinnell, Randy M. Morgenstein[#]

Department of Microbiology and Molecular Genetics, Oklahoma State University, Stillwater, OK

Running title: Gluconeogenesis and A22 resistance in *E. coli*

[#] Address correspondence to Randy Morgenstein, randy.morgentein@okstate.edu

Abstract word count: 146

Manuscript word count: 4352

Abstract

Antibiotic resistant bacteria are a global threat to human health. One way to combat the rise of antibiotic resistance is to make new antibiotics that target previously ignored proteins. The bacterial actin homolog, MreB, is highly conserved among rod-shaped bacteria and essential for growth, making MreB a good focus for antibiotic targeting. Therefore, it is imperative to understand mechanisms that can give rise to resistance to MreB targeting drugs. Using the MreB targeting drug, A22, we show that changes to central metabolism through deletion of TCA cycle genes, leads to the upregulation of gluconeogenesis resulting in cells with an increased minimal inhibitory concentration to A22. This phenotype can be recapitulated through the addition of glucose to the media. Finally, we show that this increase in minimal inhibitory concentration is not specific to A22 but can be seen in other cell wall targeting antibiotics, such as mecillinam.

Importance

The spread of antibiotic resistance has made bacterial infections harder to treat. Finding new targets for antibiotic development is critical to overcoming the variety of resistance mechanism that are already crippling our ability to treat infections with current antibiotics. The bacterial actin homolog MreB is a good target for new antibiotic development because it is essential for growth and highly conserved among rod-shaped pathogens. The significance of this research is in understanding the mechanisms cells can develop toward the inhibition of MreB to better understand how to make MreB targeting antibiotics in the future.

47 **Introduction**

48

49 The spread of antibiotic resistance among bacteria is a global human health
50 concern (1). In May 2015 the World Health Organization (WHO) outlined a global action
51 plan on antimicrobial resistance. Due to the spread of antibiotic resistance among
52 pathogens against currently used therapeutics, development of new antibiotics is
53 required (2-4). One strategy for the development of new antimicrobials is the
54 modifications of current drugs, such as has been done with the penicillin family of
55 antibiotics; however resistance to these new drugs requires the simple modification of
56 beta-lactamase enzymes (5). For example, the second-generation penicillin, methicillin,
57 was developed in 1959 with resistant strains isolated only two years later (6). Another
58 strategy is to develop new therapeutics against novel bacterial targets, for which
59 resistance has not yet been selected, which should increase the longevity of these new
60 antibiotics.

61 The bacterial actin homolog, MreB, is a highly conserved and essential protein
62 necessary for shape and growth in many rod-shaped human pathogens, including
63 *Escherichia coli, Salmonella enterica, Pseudomonas aeruginosa,* and *Vibrio cholerae*
64 (7, 8). Therefore, MreB is a good target candidate for new antibiotic development. While
65 there are no current FDA-approved MreB-targeting antibiotics, the compound A22 is
66 used in laboratory settings to study the role of MreB in the cell. A22 binds adjacent to
67 the ATP binding pocket of MreB and alters its polymerization dynamics (9-13). MreB
68 directs the localization of cell wall synthesis, and disruption of MreB, either through the
69 use of A22 or genetic modifications, causes cells to become misshapen and lyse. One

70 issue with developing A22-like compounds for human use is the high rate of suppressor
71 mutations leading to A22 resistance, which almost always map to MreB (12, 14-16).
72 Therefore, it is imperative that we understand mechanisms of resistance against MreB-
73 targeting antibiotics, including mutations outside of MreB, before exploring the
74 expensive process of MreB-targeted drug development.

75 Mutations in genes encoding enzymes of the tricarboxylic acid cyle (TCA) cycle
76 have been shown to provide antibiotic tolerance. It was shown that a mutation in *icd*,
77 which encodes isocitrate dehydrogenase, results in toxic intermediates which activate
78 efflux pumps. *icd* mutants have increased resistance to nalidixic acid (NA), a DNA-
79 targeting drug, because the intermediates that accumulate due to this mutation activate
80 the AcrAB-TolC efflux pump, which can pump NA out of the cell (17). More recently, it
81 was shown that antibiotic tolerance was induced by inhibiting ATP production (18, 19).
82 One way this could be achieved is by blocking enzymes in the TCA cycle such as
83 aconitase (*acnB*) or succinate dehydrogenase (*sdhA*), which lowers the reducing power
84 available for oxidative respiration (20). In addition to the connection between the TCA
85 cycle and antibiotic resistance, a connection between the TCA cycle and cell size has
86 been shown in *Caulobacter crescentus*. In *C. crescentus*, mutations that result in the
87 accumulation of α-ketoglutarate cause cell shape defects by reducing the synthesis of
88 cell wall precursors (21).

89 Here, we performed a screen of *E. coli* deletion mutants to find mutations that
90 caused an increase in the minimal inhibitory concentration of A22 (MIC_{A22}) in *E. coli*.
91 This screen uncovered many possible pathways that could lead to a higher MIC_{A22}.
92 Because of the well-known connection between cell shape and size and metabolism

93 and the connections between the TCA cycle and antibiotic tolerance, we focused our
94 efforts on understanding how disruption of the TCA cycle protein, Mdh, leads to a higher
95 MIC_{A22}. We show that deletion of *mdh* results in a higher MIC_{A22} through a novel
96 mechanism that activates gluconeogenesis, causing an increase in the levels of cell wall
97 precursors. Additionally, we found that this higher MIC is phenocopied by the addition of
98 glucose to the growth medium and holds true when cells are treated with mecillinam, an
99 inhibitor of the cell wall synthesis enzyme penicillin binding protein (PBP) 2.
100
101 **Results**
102
103 *Metabolic gene deletions cause an increase in MIC_{A22}.* We wanted to determine if there
104 were gene deletions that result in a cell's ability to live without the essential bacterial
105 actin homolog, MreB. It is known that mutations that cause an increase in expression of
106 the cell division genes *ftsZAQ* suppresses the growth defects of deletions of many cell
107 shape determinants, including MreB (22-24). Because suppressor mutations arise
108 quickly when *mreB* is deleted, we used the MreB depolymerizing drug A22 to mimic the
109 loss of MreB in order to determine if cells can bypass the need for MreB (25). A random
110 subset of the Keio deletion library was screened for gene deletions that cause an
111 increase in the concentration of A22 that results in less than half the growth ($O.D._{600}$)
112 compared to the LB only control (henceforth referred to as, MIC_{A22}). (26). Of the 276
113 gene deletions from the Keio collection screened, we found 86 gene deletions (31%)
114 that showed a higher MIC value than wild-type (WT) cells (Table S1). Gene ontology
115 analysis revealed that the largest class of mutants with increased MIC_{A22} were in genes

116 involved in cellular metabolism (Fig. 1A), and, of these, two were involved in the TCA
117 cycle.

118 Our initial subset of the Keio collection used in the screen contained three strains
119 with deletions in TCA cycle genes: malate dehydrogenase (*mdh*), isocitrate
120 dehydrogenase (*icd*), and fumarase (*fumE*) (Fig. 1BC). Of these, only *mdh* and *icd*
121 showed a higher MIC_{A22} than WT cells from our initial screen (Table S1). We confirmed
122 the presence of the deletion in each of these genes by PCR and retested the MIC_{A22}.
123 We found that the *mdh* deletion resulted, but not the *icd* deletion resulted in an increase
124 in the MIC_{A22} (Fig. 1B). This suggests that some of the 86 genes in table S1 are false
125 positives. However, *mdh* was found both in the initial screen and after PCR confirmation
126 to have a large increase in the MIC_{A22}.

127 FumE is not the major fumarase in *E. coli* and its function was only discovered
128 through a large-scale metabolomics screen, before which it was predicted to be a
129 transcription factor (27, 28). Because the *fumE* deletion did not show an increased
130 MIC_{A22}, we tested if deletion of the major aerobic fumarase, FumA, or other enzymes
131 involved in the TCA cycle increase the MIC_{A22} by going back to the Keio collection and
132 performing MIC assays on citrate synthase (*gltA*), aconitate hydratase (*acnB*), 2-
133 oxoglutarate dehydrogenase (*sucA*), succinyl-CoA synthetase (*sucC*),
134 succinate:quinone oxidoreductase (*sdhA*), and the major anaerobic fumarase (*fumA*)
135 after PCR confirmation of the deletions (29). Of these six tested mutants, only two
136 showed a higher MIC_{A22}: *acnB* and *sucC* (Fig 1C).

137 Previous studies have shown changes to antibiotic sensitivity when mutations are
138 made in the genes involved in the TCA cycle (17, 20, 21). *acnB* mutations are thought

139 to alter antibiotic susceptibility through changes in cellular ATP levels (19), a
140 mechanism that might explain our observations. To our knowledge, neither mutations in
141 *mdh* nor *sucC* have been reported to cause a decrease in antibiotic susceptibly. In this
142 paper, we focus our efforts on understanding the effects of the *mdh* mutation on A22
143 tolerance, as we do not expect the *mdh* mutation to function in ATP synthesis because
144 the action of Mdh occurs after the steps in the TCA cycle where reducing power is
145 created.

146 Slow growth is known to help cells grow without MreB (22). Growth curves of WT
147 and *mdh* cells show that in our test conditions (LB medium) there is no appreciable
148 change in growth rates, indicating that slow growth is not contributing to the increase in
149 MIC_{A22} (Fig. S1) and that ATP production is not severely affected in this strain. Because
150 the growth rate was the same between WT and *mdh* cells and increased tolerance to
151 A22 is not a universal feature of TCA cycle gene deletions (Fig. 1BC), we hypothesize
152 that the Mdh enzyme or changes in malate levels (the substrate of Mdh) is the most
153 likely cause of the increased MIC_{A22} seen in the *mdh* mutant.

154

155 *A22 disrupts MreB in mdh cells.* Cells could show an increased MIC_{A22} for three
156 reasons: 1) A22 cannot accumulate in the cell to appropriate concentrations, 2) A22
157 cannot enter the cell due to membrane changes, or 3) MreB polymers are protected
158 from A22. With respect to the first option, it is possible that an intermediate accumulates
159 in the *mdh* mutant that activates an efflux pump that removes A22 from the cells or that
160 A22 is degraded faster in *mdh* cells due to changes in the metabolic activity of different
161 enzymes. To determine if any of the above mechanisms are the cause for the increased

162 MIC_{A22} in *mdh* cells, we imaged WT cells, an MreB point mutant resistant to A22, and
163 *mdh* cells after growth in LB alone, LB with a sublethal concentration of A22 (1 µg/ml)
164 for 4 hours, or LB spiked with 10 µg/ml of A22 for 2 hours after 2 hours of growth. As
165 expected, both A22 treatments cause WT cells to become round, whereas the MreB
166 point mutant remains as a rod regardless of A22 treatment (16). However, *mdh* cells
167 became round, like WT cells, confirming that A22 is able to accumulate in the mutant
168 cells at a high enough concentration to inhibit MreB polymers (Fig. 2S). These data
169 further suggest that either Mdh or malate levels are responsible for the increased
170 MIC_{A22}.
171 *mdh mutants up-regulate gluconeogenesis leading to an increase in* MIC_{A22}. There is
172 precedent for metabolic proteins having additional cellular roles separate from their
173 known enzymatic activities (moonlighting). For example, aconitase, an enzyme in the
174 TCA cycle, that forms D-*threo*-isocitrate from citrate with aconitate as an intermediate,
175 also plays a role in iron sensing regulation by binding to specific mRNAs for post-
176 transcriptional regulation (30, 31). Additional moonlighting enzymes have been shown
177 to help regulate cell shape/size based on changes in nutrient availability (recently
178 reviewed (32, 33)). An example in *E. coli* is OpgH, a metabolic enzyme which can
179 directly interact with the main division protein, FtsZ, to help modulate cell length in
180 different nutrient conditions (34).
181 As a deletion of *mdh* would inhibit both its normal enzymatic function and any
182 moonlighting activity, we performed metabolomic analysis to identify changes in
183 metabolites in *mdh* cells to determine if these changes affect the MIC_{A22}. Malate levels
184 act as a positive control in these experiments, as malate should be increased in cells

185 with a defective malate dehydrogenase. As expected, malate levels were higher in the
186 *mdh* mutant than WT cells (Fig. 2A). In the *mdh* mutant, the increased levels of malate
187 should increase flux into pyruvate through malate dehydrogenase (*maeAB*), which is
188 observed by elevated pyruvate levels in the *mdh* mutant (Fig. 2B). This increase in
189 pyruvate could either flow back into the TCA cycle or into gluconeogenesis to produce
190 sugar (35). We saw an increase in glucose-6-phosphate (G6P), the end product of
191 gluconeogenesis, in the *mdh* mutant, which could only come from increased
192 gluconeogenesis because the cells were grown in LB medium without any sugar (Fig.
193 2C). G6P can be converted into fructose-6-phosphate which can be used to form N-
194 acetylglucosamine (NAG), while pyruvate can be converted to phosphoenolpyruvate,
195 another metabolite used in the synthesis of cell wall precursors (36).
196 Thus, the increased levels of both G6P and pyruvate led us to hypothesize that
197 the *mdh* deletion causes an increase in gluconeogenesis resulting in increased levels of
198 cell wall precursor which may cause an increase in cell wall synthesis (37). To this end,
199 we looked for changes in the level of cell wall precursors in the metabolomics data and
200 saw an increase in UDP-NAG, confirming our hypothesis (Fig. 2D). These results
201 suggest that increasing the amount of cell wall precursors can suppress the lethal
202 effects of MreB disruption and that there is not a moonlighting function of Mdh.
203 *The addition of glucose mimics deletion of mdh.* To confirm our hypothesis that the
204 increase of cell wall precursors caused by an increase in gluconeogenesis is the reason
205 for a higher MIC_{A22}, we sought to increase cell wall precursor synthesis through another
206 mechanism. Because G6P levels were increased in *mdh* cells, we reasoned that the
207 addition of glucose to the medium would have a similar effect on the levels of cell wall

208 precursors as deleting *mdh*. Additionally, glucose has been shown to compensate for
209 mutations in aconitase to restore antibiotic susceptibility (20).
210 MIC assays were performed on WT cells grown on LB medium with increasing
211 amounts of glucose or α-methyl-D-glucoside (αMG), a nonhydrolyzable form of glucose
212 (38, 39). While very low levels (<0.125%) of glucose had no effect on the MIC_{A22} in WT
213 cells, even glucose levels as low as 0.125% resulted in a statistically significant increase
214 in the fold change of the MIC_{A22} in cells grown with glucose vs LB alone compared with
215 cells grown with αMG vs LB (Fig. 3). An increase in the glucose levels resulted in even
216 higher MIC_{A22} fold changes. The significant increase in MIC_{A22} during glucose versus
217 αMG treatment suggests that the changes are not due to osmotic protection caused by
218 the sugar. These results further support our hypothesis that increasing the levels of cell
219 wall precursors leads to an increase in MIC_{A22}.
220
221 *Deletion of mdh leads to an increased MIC to mecillinam.* The major role of MreB is to
222 direct the location of the cell wall synthesis enzymes. It has been suggested that MreB
223 forms a complex with the SEDS family of cell wall synthesis enzymes (40-42).
224 Specifically, recent work has suggested that MreB interacts with RodA and PBP2 to
225 regulate cell elongation, while PBP1A/1B work independently of MreB (40). Because the
226 *mdh* deletion results in cells with a higher MIC_{A22}, it stands to reason that cells might
227 also have a higher MIC against mecillinam, a PBP2-targeting antibiotic (43). To that end,
228 we performed MIC assays on mecillinam and other antibiotics that target cell wall
229 synthesis proteins to determine how general the effects of the *mdh* deletion are on the
230 MICs of cell wall-targeting drugs.

231 We performed MIC assays with a variety of cell wall-targeting antibiotics that
232 inhibit either cell elongation (ampicillin, mecillinam, cefsulodin) or cell division
233 (cephalexin), by blocking the activity of different PBPs involved in cell wall synthesis. An
234 MIC fold change >1 indicates that the *mdh* deletion causes cells to be more resistant
235 and a fold change <1 indicates that WT cells are more sensitive to the specified
236 antibiotic. The only other cell wall-targeting antibiotic to which the *mdh* deletion shows
237 an increased MIC is mecillinam, which targets the MreB complex partner PBP2 (Fig. 4).
238 The fact that the *mdh* deletion strain does not have a higher MIC_{cef} adds more evidence
239 that PBP1A/B are not part of the MreB complex because cefsulodin specifically targets
240 PBP1A/1B. Cephalexin targets PBP3 (FtsI) which is part of the division machinery, a
241 different complex than the MreB-elongosome. We did not see an increase in the MIC_{ceph}
242 in the *mdh* deletion, suggesting that an increase in gluconeogenesis cannot overcome
243 cell division inhibition. Ampicillin targets multiple PBPs, with the highest affinity for
244 PBP4, PBP3, and PBP2 in that order (44, 45). Because ampicillin binds to PBP3 tightly
245 and there was no increase in the MIC_{Ceph}, it leads to reason that deletion of *mdh* would
246 not have an effect on the MIC_{Amp}. These results suggest that the up-regulation of
247 gluconeogenesis caused by the *mdh* deletion specifically causes an increase to the MIC
248 of drugs that target the MreB elongation synthesis complex (A22 and mecillinam), but
249 not to other cell wall-targeting antibiotics.
250 Inactivation of aconitase (*acnB*) and succinyl-CoA synthetase (*sucC*), leads to an
251 increase in the MIC_{A22} (Fig. 1D); therefore, we tested whether deletions of these genes
252 also leads to an increase in the MIC_{mec}. The *acnB* mutation displays an increased
253 MIC_{mec}, while deletion of *sucC* does not (Fig. 3S). This suggests that the role of SucC in

254 A22 resistance is different than that of Mdh. However, it is unclear if AcnB acts through
255 a general antibiotic resistance mechanism via ATP depletion or through a specific
256 MreB-elongosome mechanism.
257
258 *Up-regulation of gluconeogenesis leads to an increased MIC to mecillinam.* The addition
259 of glucose to the media was able to phenocopy the effects of deleting *mdh* on the
260 MIC_{A22} (Fig. 3). Because we saw a similar increase in the MIC_{Mec} as we saw with the
261 MIC_{A22} in the *mdh* deletion, we wanted to confirm that the addition of glucose would also
262 lead to an increased MIC_{Mec} in WT cells. The addition of glucose leads to a statistically
263 significant increase in the MIC_{Mec} versus αMG (Fig. 3). Taken together, these data
264 indicate that an increase in cell wall precursors, either through an increase in
265 gluconeogenesis or the addition of glucose to the medium, leads to an increased MIC of
266 antibiotics that specifically target the MreB elongosome, but not other cell wall synthesis
267 enzymes.
268
269 **Discussion**
270 Our findings demonstrate that changes in cellular metabolism can have drastic
271 effects on antibiotic resistance. An increase in gluconeogenesis, through mutations of
272 metabolic enzymes or the addition of glucose to the growth medium, leads to increased
273 MICs of both the MreB targeting drug, A22, and the PBP2-targeting drug, mecillinam.
274 This effect appears to be specific for the MreB cell wall synthesis complex as we do not
275 see an increase in MIC of antibiotics that target other enzymes in the cell wall synthesis
276 pathway.

277 Cellular metabolism is a complicated and interconnected network. It is difficult to
278 predict how mutations in one pathway may lead to changes in other pathways in a cell.
279 While trying to understand novel mechanisms for A22 resistance, we found that loss of
280 MDH, an enzyme in the TCA cycle, leads to an increase in the MIC_{A22} by inducing
281 gluconeogenesis (Fig. 1). The induction of gluconeogenesis leads to the overproduction
282 of cell wall precursors (Fig. 3). MreB is thought to control where cell wall synthesis
283 occurs, with the localization of MreB, enriched in the middle of the cell, correlating with
284 the sites of new cell wall growth in *E. coli* (46, 47). When MreB is disrupted, the location
285 of cell wall synthesis becomes random, causing misshapen cells and eventually cell
286 death due to lysis (46, 48, 49). We hypothesize that the increase in cell wall precursors
287 allows for more cell wall synthesis and cell survival by prohibiting cell lysis. The fact that
288 both inhibition of MreB with PBP2 is suppressed through this mechanism, suggests that
289 the increase in cell wall precursors allows for a secondary synthesis system to dominate
290 (see below). Below, we discuss the implications for these results on understanding
291 bacterial cell wall synthesis and the development of drug treatment plans.
292

293 **MreB is complexed with PBP2 but not class A PBPs.**

294 The bacterial cell wall is a macromolecule made up of sugars crosslinked by
295 proteins to provide shape and support to the cell. In rod-shaped bacteria, such as *E.*
296 *coli, B. subtilis, and C. cresentus,* MreB is thought to form the main protein of the
297 elongosome complex consisting of multiple PBPs, MreBCD, RodA, and RodZ. Work in
298 the above species led to the hypothesis that MreB interacts with the cytoplasmic cell
299 wall synthesis components and helps to direct the localization of the periplasmic-acting

300 enzymes (16, 23, 46, 50-54). MreB is a cytoplasmic protein that is associated with the
301 inner face of the cytoplasmic membrane (9). How does this cytoplasmic protein
302 communicate with the extracellular cell wall? Our recent work showed that the integral
303 membrane protein RodZ acts as a linker between MreB and the cell wall synthesis
304 machinery, enabling MreB dynamics and assembly (16, 47). When *rodZ* is deleted, cells
305 grow as irregular round cells because the localization of MreB and the number of MreB
306 polymers are disrupted.

307 Recent work has questioned the model that the MreB elongosome is a large
308 complex composed of both the bifunctional class A PBPs (aPBPs), and monofunctional
309 class B PBPs (bPBPs). The aPBPs contain both transglycosylation and transpeptidation
310 activities, and thus should be functional alone, while the bPBPs, such as PBP2,
311 possess only transpeptidation activity. However, PBP2 is essential in *E. coli*, and in both
312 *B. subtilis* and *E. coli*, cell elongation has been shown to proceed without the aPBPs
313 (40, 42). This suggests that the MreB complex is not as large as previously thought. If
314 bPBPs can cause cell elongation without aPBPs, then there must be another enzyme
315 capable of transglycosylation reactions. RodA has been suggested to be the
316 transglycosylase that works with PBP2 (bPBP) (40, 42). These authors also showed
317 that the RodA-PBP2 complex works with the MreB cytoskeleton while the aPBPs act
318 separately from this complex. Our previous work studying MreB dynamics suggested
319 that RodZ helps modulate MreB motion through interactions with RodA/PBP2, further
320 confirming the idea that they are in a complex together (16). Here we show that
321 resistance to antibiotics that target MreB (A22) or PBP2 (mecillinam), but not aPBPs
322 (cefsulodin) are less effective when gluconeogenesis is upregulated (Fig. 3-4).

323 The results together reinforce the model that MreB forms a cell wall synthesis
324 complex with PBP2 but not PBP1A/B, and suggest that cell wall synthesis deriving from
325 the activity of aPBPs may be upregulated when there is an abundance of precursor
326 molecules in the cell. Upregulation of an aPBP-specific synthesis mechanism would
327 explain how cells can grow when MreB or PBP2 are inhibited. How aPBP activity is
328 modulated when other cell wall synthesis mechanisms are inhibited is currently not
329 known but would be an interesting topic for further study.
330
331 **Drug efficacy is affected by the metabolic state of cells.**
332 Because antibiotic resistance is more prevalent now than ever before, it is
333 essential that we understand how and when to use the antibiotics to which bacteria are
334 susceptible. Antibiotic resistance normally comes from genetic changes in a cell. This
335 can be through the acquisition of degrading enzymes, such as beta-lactamases for
336 resistance to penicillins; the modification of a drug target, such as mutations of the *rpsL*
337 gene for resistance to streptomycin; or a cell's ability to limit the intracellular
338 concentration of an antibiotic, such as through upregulation of efflux pumps (55-57).
339 The efficacy of antibiotics is higher against growing cells, as slow growing cells show an
340 increase tolerance to many antibiotics (58, 59). When only a subfraction of the
341 population is tolerant to antibiotic exposure, the surviving cells are termed 'persisters'
342 (60).
343 Here we show that mutations in metabolic genes such as *mdh,* seemingly
344 unrelated to the target of both the antibiotics, A22 and mecillinam, leads to increases in
345 antibiotic susceptibility (Fig.1 and 4). Additionally, the addition of glucose to the growth

346 media phenocopies the *mdh* mutation and leads to an increase in the MIC of both
347 drugs. Previous research has shown that while persister cells are more tolerant of
348 aminoglycoside antibiotics, the addition of different sugars specifically potentiated the
349 effects of gentamycin and other aminoglycosides, resulting in a reduction of persister
350 cell survival after treatment (61). The work presented here suggests that the addition of
351 sugar has the opposite effect on the efficacy of mecillinam and decreases its
352 effectiveness. Additionally, inhibiting ATP production can lead to increases in antibiotic
353 tolerance which can be bypassed through the addition of glucose (18-20).Therefore, it
354 will be imperative when designing an antibiotic treatment protocol that one remembers
355 that there is not a single solution. While the addition of sugars may help to treat cells
356 when using aminoglycosides by killing both actively growing cells and persister cells, we
357 show the opposite is true when using mecillinam, as the addition of sugar actually
358 increases the required dose (MIC).

359 Furthermore, gluconeogenic metabolism has been shown to promote infection.
360 Colonization by *E. coli* of both cows and mice has been shown to increase during
361 gluconeogenic growth, especially when undergoing competition in the gut (62, 63).
362 Moreover, a gluconeogenic environment leads to an increase in virulence factor
363 expression of enterohemorrhagic *E. coli* (64). Therefore, the use of metabolites to
364 potentially help eliminate a subset of cells, such as persister cells, may have the
365 unintended consequences of both increasing colonization and virulence of other cells,
366 and diminishing the efficacy of other antibiotics.

367 The properties that make MreB an attractive drug target — conservation across
368 many pathogens and essentiality — are true for other members of the MreB complex,

369 including RodA and RodZ. Our results suggest that drugs that target these proteins
370 would be less effective if gluconeogenesis is activated. As new antibiotics are
371 developed against novel targets, these results show it is important to think about the
372 broad function of the target protein as the efficacy of a drug may be affected in
373 seemingly unknown ways as we have shown that antibiotics tolerance to MreB can be
374 increased through a mutation in the TCA cycle gene *mdh*.
375
376 **Material and Methods**
377
378 **Bacterial Growth.** Bacteria were grown using standard laboratory conditions. Cultures
379 were grown overnight in LB medium (10g/L NaCl, 10g/L tryptone, 5g/L yeast extract)
380 and subcultured in the morning 1:1000 and grown to exponential phase ($O.D._{600}$ 0.3-0.6)
381 at 37°C. Keio collection mutants were moved in MG1655 using P1 transduction.
382 Transductants were selected for on Kanamycin (30µg/mL) and confirmed by PCR.
383
384 **MIC assay.**
385 Optical densities of all cultures used in the minimum inhibitory concentration assays
386 (MIC) were checked at 600 nm (OD_{600}) with a Thermo Scientific Biomate-3S. Overnight
387 cultures were grown in LB and normalized to the same starting OD_{600}. 1:100 dilutions
388 were made into 96-well plates filled with 100ul of LB medium plus indicated antibiotics
389 and/or specified sugars and tricarboxylic acids. Two-fold dilutions of each antibiotic was
390 made.
391
392 **Microscopy.**

393 For all imaging, cells were grown at 37°C in LB medium. Imaging was done on 1% LB-
394 agarose pads at room temperature. Phase contrast images were collected on a Nikon
395 Ni-E epifluorescent microscope equipped with a 100X/1.45 NA objective (Nikon), Zyla
396 4.2 plus cooled sCMOS camera (Andor), and NIS Elements software (Nikon).
397
398 **Metabolomics.**
399 **Collection.** Cells were grown overnight in LB medium and then subcultured 1:1000 in
400 fresh LB for ~4 hours until in exponential phase. Cells were passed through a filter and
401 quenched with cold acetonitrile:methanol:water (40:40:20) + 0.5% formic acid. The
402 solution was neutralized with 1.9M ammonium bicarbonate before being centrifuged for
403 5 minutes. Supernatants were collected for mass spectrometry
404 **Analysis.** Supernatants were analyzed via the methods of Su et al. (65). Specificity was
405 achieved through a combination of chromatographic separations followed by high-
406 resolution MS. This method allows for the identification of ~300 water soluble
407 metabolites. Covariant ion analysis (COVINA) was used to identify peaks.
408
409 **Acknowledgements**
410 Research reported in this publication was supported by NIGMS of the National Institutes
411 of Health under award number R15GM129636-01A1. 100% of this project was financed
412 with Federal money. The content is solely the responsibility of the authors and does not
413 necessarily represent the official view of the NIH.
414

The authors would like to thank Dr. Elizabeth Ohneck and Dr. Tyrrell Conway for editing of the manuscript.

1. W. H. O. (WHO) (Antimicrobial Resistance: Global Report on Surveillance. ed WHO (Geneva, Switzerland).
2. S. A. McEwen, P. J. Collignon, Antimicrobial Resistance: a One Health Perspective. *Microbiology Spectrum* **6** (2018).
3. A. Pragasam, B. Veeraraghavan, E. Nalini, S. Anandan, K. Kaye, An Update on Antimicrobial Resistance and the Role of Newer Antimicrobial Agents for *Pseudomonas aeruginosa*. *Indian Journal of Medical Microbiology* **36**, 303-316 (2018).
4. S. Lakhundi, K. Zhang, Methicillin-Resistant *Staphylococcus aureus*: Molecular Characterization, Evolution, and Epidemiology. *Clinical Microbiology Reviews* **31**, e00020-00018 (2018).
5. S. S. Castle, "Penicillins" in xPharm: The Comprehensive Pharmacology Reference, S. J. Enna, D. B. Bylund, Eds. (Elsevier, New York, 2007), pp. 1-3.
6. M. Lobanovska, G. Pilla, Penicillin's Discovery and Antibiotic Resistance: Lessons for the Future? *The Yale journal of biology and medicine* **90**, 135-145 (2017).
7. F. van den Ent, L. A. Amos, J. Lowe, Prokaryotic Origin of the Actin Cytoskeleton. *Nature* **413**, 39-44 (2001).
8. S. A. Alyahya *et al.*, RodZ, a Component of the Bacterial Core Morphogenic Apparatus. *Proceedings of the National Academy of Sciences* **106**, 1239-1244 (2009).

436 9. F. van den Ent, T. Izoré, T. B. Bharat, C. M. Johnson, J. Lowe, Bacterial Actin MreB Forms
437 Antiparallel Double Filaments. *eLife* **3** (2014).
438 10. E. Awuni, Y. Mu, Effect of A22 on the Conformation of Bacterial Actin MreB.
439 *International journal of molecular sciences* **20**, 1304 (2019).
440 11. Y. Awuni, S. Jiang, R. C. Robinson, Y. Mu, Exploring the A22-Bacterial Actin MreB
441 Interaction through Molecular Dynamics Simulations. *The Journal of Physical Chemistry*
442 *B* **120**, 9867-9874 (2016).
443 12. Z. Gitai, N. A. Dye, A. Reisenauer, M. Wachi, L. Shapiro, MreB Actin-Mediated
444 Segregation of a Specific Region of a Bacterial Chromosome. *Cell* **120**, 329-341 (2005).
445 13. G. J. Bean *et al.*, A22 Disrupts the Bacterial Actin Cytoskeleton by Directly Binding and
446 Inducing a Low-Affinity State in MreB. *Biochemistry* **48**, 4852-4857 (2009).
447 14. N. Ouzounov *et al.*, MreB Orientation Correlates with Cell Diameter in *Escherichia coli*.
448 *Biophysical Journal* **111**, 1035-1043 (2016).
449 15. N. A. Dye, Z. Pincus, I. C. Fisher, L. Shapiro, J. A. Theriot, Mutations in the Nucleotide
450 Binding Pocket of MreB can Alter Cell Curvature and Polar Morphology in *Caulobacter*.
451 *Molecular Microbiology* **81**, 368-394 (2011).
452 16. R. M. Morgenstein *et al.*, RodZ links MreB to Cell Wall Synthesis to Mediate MreB
453 Rotation and Robust Morphogenesis. *Proceedings of the National Academy of Sciences*,
454 12510-12515 (2015).
455 17. R. B. Helling *et al.*, Toxic Waste Disposal in *Escherichia coli*. *Journal of bacteriology* **184**,
456 3699-3703 (2002).

457 18. Y. Shan *et al.*, ATP-Dependent Persister Formation in *Escherichia coli*. *mBio* **8**, e02267-
458 02216 (2017).
459 19. B. P. Conlon *et al.*, Persister Formation in *Staphylococcus aureus* is Associated with ATP
460 Depletion. *Nature Microbiology* **1**, 16051 (2016).
461 20. S. E. Rowe *et al.*, Reactive Oxygen Species Induce Antibiotic Tolerance During Systemic
462 *Staphylococcus aureus* Infection. *Nature Microbiology* **5**, 282-290 (2020).
463 21. I. Irnov *et al.*, Crosstalk Between the Tricarboxylic Acid Cycle and Peptidoglycan
464 Synthesis in *Caulobacter crescentus* through the Homeostatic Control of α-
465 ketoglutarate. *PLoS genetics* **13**, e1006978-e1006978 (2017).
466 22. F. O. Bendezú, P. A. J. de Boer, Conditional Lethality, Division Defects, Membrane
467 Involution, and Endocytosis in *mre* and *mrd* Shape Mutants of *Escherichia coli*. *Journal of*
468 *Bacteriology* **190**, 1792-1811 (2008).
469 23. T. Kruse, J. Bork-Jensen, K. Gerdes, The Morphogenetic MreBCD Proteins of *Escherichia*
470 *coli* form an Essential Membrane-Bound Complex. *Molecular Microbiology* **55**, 78-89
471 (2005).
472 24. D. Vinella, D. Joseleau-Petit, D. Thévenet, P. Bouloc, R. D'Ari, Penicillin-binding Protein 2
473 Inactivation in *Escherichia coli* Results in Cell Division Inhibition, Which is Relieved by
474 FtsZ Overexpression. *Journal of bacteriology* **175**, 6704-6710 (1993).
475 25. N. Iwai, K. Nagai, M. Wachi, Novel S-Benzylisothiourea Compound That Induces
476 Spherical Cells in Escherichia coli Probably by Acting on a Rod-shape-determining
477 Protein(s) Other Than Penicillin-binding Protein 2. *Bioscience, Biotechnology, and*
478 *Biochemistry* **66**, 2658-2662 (2002).

479 26. T. Baba *et al.*, Construction of *Escherichia coli* K-12 in-frame, Single-gene Knockout
480 Mutants: the Keio Collection. *Molecular Systems Biology* **2**, 2006.0008-2006.0008
481 (2006).
482 27. D. C. Sévin, T. Fuhrer, N. Zamboni, U. Sauer, Nontargeted *in vitro* Metabolomics for
483 High-throughput Identification of Novel Enzymes in *Escherichia coli*. *Nature Methods* **14**,
484 187-194 (2017).
485 28. E. Flores-Bautista, C. L. Cronick, A. R. Fersaca, M. A. Martinez-Nuñez, E. Perez-Rueda,
486 Functional Prediction of Hypothetical Transcription Factors of *Escherichia coli* K-12
487 Based on Expression Data. *Computational and Structural Biotechnology Journal* **16**, 157-
488 166 (2018).
489 29. C.-P. Tseng, Regulation of Fumarase (f*umB*) Gene Expression in *Escherichia coli* in
490 Response to Oxygen, Iron and Heme Availability: Role of the *arcA*, *fur*, and *hemA* Gene
491 Products. *FEMS Microbiology Letters* **157**, 67-72 (1997).
492 30. J.-A. M. Benjamin, E. Massé, The iron-sensing aconitase B binds its own mRNA to
493 prevent sRNA-induced mRNA cleavage. *Nucleic acids research* **42**, 10023-10036 (2014).
494 31. Y. Tang, J. R. Guest, Direct Evidence for mRNA Binding and Post-transcriptional
495 Regulation by *Escherichia coli* Aconitases. *Microbiology* **145**, 3069-3079 (1999).
496 32. C. S. Westfall, P. A. Levin, Bacterial Cell Size: Multifactorial and Multifaceted. *Annual*
497 *review of microbiology* **71**, 499-517 (2017).
498 33. A. M. Sperber, J. K. Herman, Metabolism Shapes the Cell. *Journal of Bacteriology* **199**,
499 e00039-00017 (2017).

500 34. N. S. Hill, P. J. Buske, Y. Shi, P. A. Levin, A Moonlighting Enzyme Links Escherichia coli Cell
501 Size with Central Metabolism. *PLOS Genetics* **9**, e1003663 (2013).
502 35. U. Sauer, B. J. Eikmanns, The PEP–pyruvate–oxaloacetate Node as the Switch Point for
503 Carbon Flux Distribution in Bacteria. *FEMS Microbiology Reviews* **29**, 765-794 (2005).
504 36. H. Barreteau *et al.*, Cytoplasmic Steps of Peptidoglycan Biosynthesis. *FEMS Microbiology*
505 *Reviews* **32**, 168-207 (2008).
506 37. D. Mengin-Lecreulx, B. Flouret, J. van Heijenoort, Pool Levels of UDP N-
507 acetylglucosamine and UDP N-acetylglucosamine-enolpyruvate in *Escherichia coli* and
508 Correlation with Peptidoglycan Synthesis. *Journal of Bacteriology* **154**, 1284-1290
509 (1983).
510 38. D. Rogers, S.-H. Yu, Substrate Specificity of a Glucose Permease of *Escherichia coli*.
511 *Journal of Bacteriology* **84**, 877-881 (1962).
512 39. M. Hernandez-Asensio, J. M. Ramirez, F. F. Del Campo, The Control by Respiration of the
513 Uptake of α-methyl-glucoside in *Escherichia coli* K12. *Archives of Microbiology* **103**, 155-
514 162 (1975).
515 40. H. Cho *et al.*, Bacterial Cell Wall Biogenesis is Mediated by SEDS and PBP Polymerase
516 Families Functioning Semi-Autonomously. *Nature Microbiology* **1**, 16172 (2016).
517 41. S. Leclercq *et al.*, Interplay Between Penicillin-binding Proteins and SEDS Proteins
518 Promotes Bacterial Cell Wall Synthesis. *Scientific Reports* **7**, 43306 (2017).
519 42. A. J. Meeske *et al.*, SEDS Proteins are a Widespread Family of Bacterial Cell Wall
520 Polymerases. *Nature* **537**, 634-638 (2016).

521 43. B. G. Spratt, The Mechanism of Action of Mecillinam. *Journal of Antimicrobial*
522 *Chemotherapy* **3**, 13-19 (1977).
523 44. D. A. Preston, C. Y. Wu, L. C. Blaszczak, D. E. Seitz, N. G. Halligan, Biological
524 Characterization of a New Radioactive Labeling Reagent for Bacterial Penicillin-binding
525 Proteins. *Antimicrobial agents and chemotherapy* **34**, 718-721 (1990).
526 45. N. A. Curtis, D. Orr, G. W. Ross, M. G. Boulton, Affinities of Penicillins and
527 Cephalosporins for the Penicillin-binding Proteins of *Escherichia coli* K-12 and their
528 Antibacterial Activity. *Antimicrobial agents and chemotherapy* **16**, 533-539 (1979).
529 46. T. S. Ursell *et al.*, Rod-Like Bacterial Shape is Maintained by Feedback Between Cell
530 Curvature and Cytoskeletal Localization. *Proceedings of the National Academy of*
531 *Sciences* **111**, E1025-E1034 (2014).
532 47. B. P. Bratton, J. W. Shaevitz, Z. Gitai, R. M. Morgenstein, MreB Polymers and Curvature
533 Localization are Enhanced by RodZ and Predict *E. coli's* Cylindrical Uniformity. *Nature*
534 *Communications* **9**, 2797 (2018).
535 48. S. Wang, Ned S. Wingreen, Cell Shape Can Mediate the Spatial Organization of the
536 Bacterial Cytoskeleton. *Biophysical Journal* **104**, 541-552 (2013).
537 49. L. Furchtgott, N. S. Wingreen, K. C. Huang, Mechanisms for Maintaining Cell Shape in
538 Rod-Shaped Gram-negatve Bacteria. *Molecular Microbiology* **81**, 340-353 (2011).
539 50. C. L. White, A. Kitich, J. W. Gober, Positioning Cell Wall Synthetic Complexes by the
540 Bacterial Morphogenetic Proteins MreB and MreD. *Molecular Microbiology* **76**, 616-633
541 (2010).

542 51. A. V. Divakaruni, C. Baida, C. L. White, J. W. Gober, The Cell Shape Proteins MreB and
543 MreC Control Cell Morphogenesis by Positioning Cell Wall Synthetic Complexes.
544 *Molecular Microbiology* **66**, 174-188 (2007).
545 52. A. V. Divakaruni, R. R. O. Loo, Y. Xie, J. A. Loo, J. W. Gober, The Cell-shape Protein MreC
546 Interacts with Extracytoplasmic Proteins Including Cell Wall Assembly Complexes in
547 *Caulobacter crescentus*. *Proceedings of the National Academy of Sciences of the United*
548 *States of America* **102**, 18602-18607 (2005).
549 53. R. M. Figge, A. V. Divakaruni, J. W. Gober, MreB, the Cell Shape-Determining Bacterial
550 Actin Homologue, Co-Ordinates Cell Wall Morphogenesis in *Caulobacter crescentus*.
551 *Molecular Microbiology* **51**, 1321-1332 (2004).
552 54. Y. Kawai, R. A. Daniel, J. Errington, Regulation of Cell Wall Morphogenesis in *Bacillus*
553 *subtilis* by Recruitment of PBP1 to the MreB Helix. *Molecular Microbiology* **71**, 1131-
554 1144 (2009).
555 55. N. Honoré, S. T. Cole, Streptomycin Resistance in Mycobacteria. *Antimicrobial Agents*
556 *and Chemotherapy* **38**, 238-242 (1994).
557 56. R. Cantón *et al.*, Prevalence and Spread of Extended-spectrum β-lactamase-producing
558 *Enterobacteriaceae* in Europe. *Clinical Microbiology and Infection* **14**, 144-153 (2008).
559 57. M. A. Webber, L. J. V. Piddock, The Importance of Efflux Pumps in Bacterial Antibiotic
560 Resistance. *Journal of Antimicrobial Chemotherapy* **51**, 9-11 (2003).
561 58. E. Tuomanen, R. Cozens, W. Tosch, O. Zak, A. Tomasz, The Rate of Killing of *Escherichia*
562 *coli* by β-Lactam Antibiotics Is Strictly Proportional to the Rate of Bacterial Growth Free.
563 *Journal of general microbiology* **132** (1986).

564 59. M. H. Pontes, E. A. Groisman, Slow Growth Determines Nonheritable Antibiotic
565 Resistance in *Salmonella enterica*. *Science Signaling* **12**, eaax3938 (2019).
566 60. A. Brauner, O. Fridman, O. Gefen, N. Q. Balaban, Distinguishing Between Resistance,
567 Tolerance and Persistence to Antibiotic Treatment. *Nature Reviews Microbiology* **14**,
568 320-330 (2016).
569 61. K. R. Allison, M. P. Brynildsen, J. J. Collins, Metabolite-enabled Rradication of Bacterial
570 Persisters by Aminoglycosides. *Nature* **473**, 216-220 (2011).
571 62. R. L. Miranda *et al.*, Glycolytic and Gluconeogenic Growth of *Escherichia coli* O157:H7
572 (EDL933) and *E. coli* K-12 (MG1655) in the Mouse Intestine. *Infection and Immunity* **72**,
573 1666-1676 (2004).
574 63. Y. Bertin *et al.*, The Gluconeogenesis Pathway is Involved in Maintenance of
575 Enterohaemorrhagic *Escherichia coli* O157:H7 in Bovine Intestinal Content. *PloS one* **9**,
576 e98367-e98367 (2014).
577 64. J. W. Njoroge, Y. Nguyen, M. M. Curtis, C. G. Moreira, V. Sperandio, Virulence Meets
578 Metabolism: Cra and KdpE Gene Regulation in Enterohemorrhagic *Escherichia coli*. *mBio*
579 **3**, e00280-00212 (2012).
580 65. X. Su *et al.*, In-Source CID Ramping and Covariant Ion Analysis of Hydrophilic Interaction
581 Chromatography Metabolomics. *Anal Chem* **92**, 4829-4837 (2020).
582
583
584
585

586

587

588

589

590

591

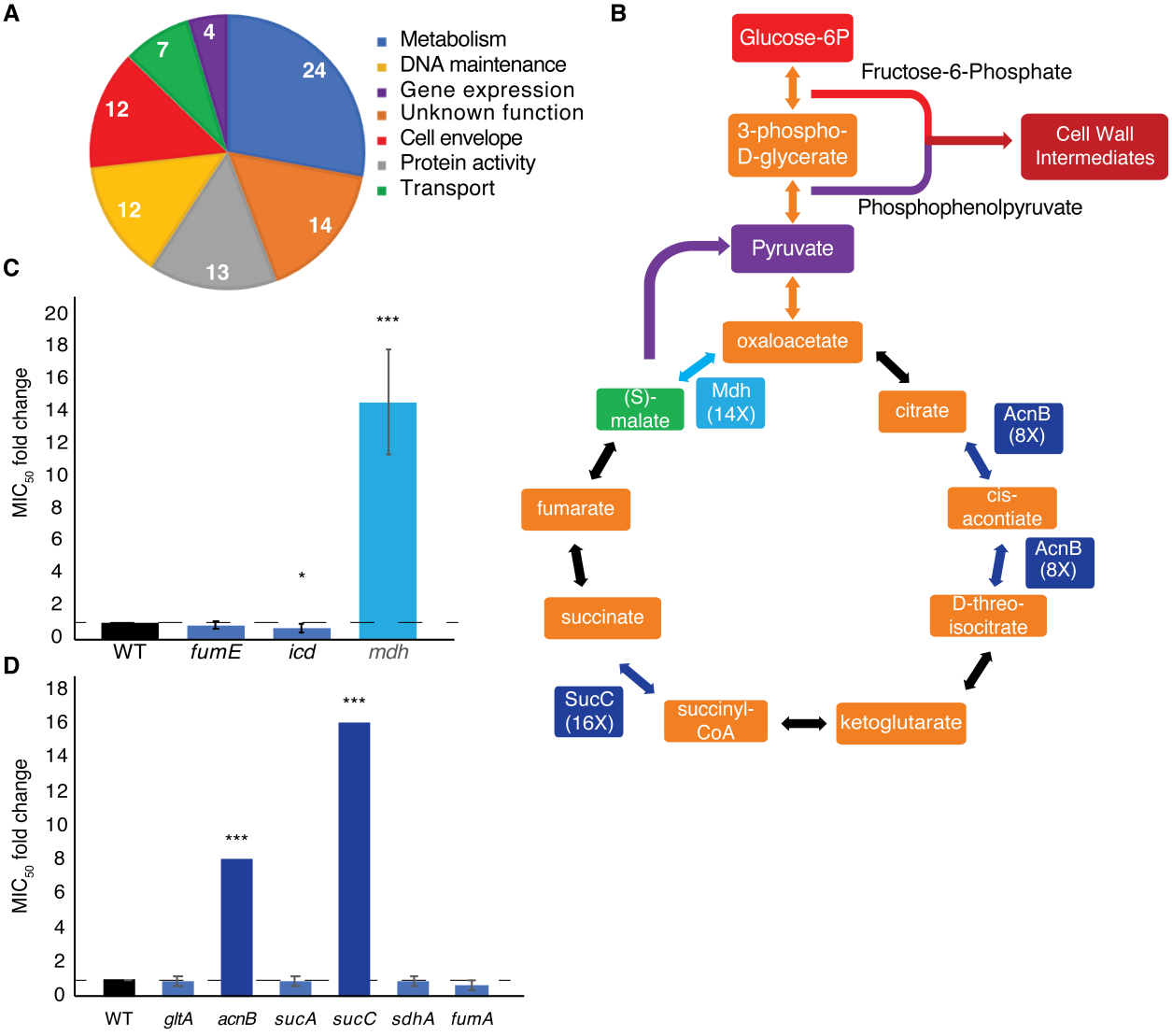

592

593

594 **Figure 1.** Mutations in the genes of the TCA cycle increase the MIC of A22. A)

595 Screening of a subset of the Keio deletion library for mutants with increased MIC_{A22}

596 yielded 86 mutations in different gene ontology groups. B) Model of the TCA cycle.

597 Indicated proteins have higher MIC_{A22} when deleted. C) MIC_{A22} of mutants from the

598 initial screen. Only *mdh* mutants show an increased MIC_{A22}. D) MIC_{A22} of mutants that

599 break the other steps in the TCA cycle. *acnB* and *sucC* deletions also show a higher

600 MIC_{A22}. MIC fold change is represented as mutant/wild-type cells. A fold change of 1

601 (dotted line) indicates no change. * p<.05, *** p>.001 comparing each strain to 1.

602

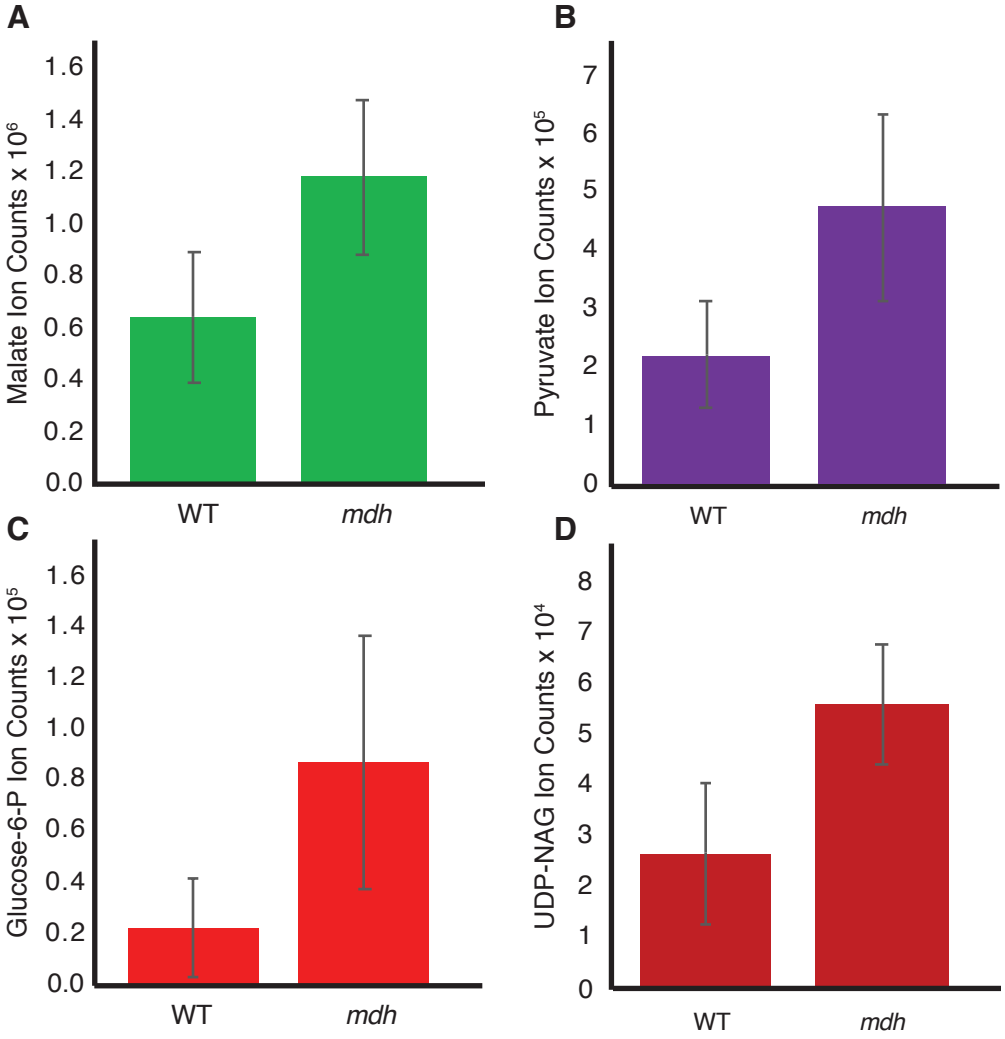

603

604 **Figure 2.** Metabolomics analysis reveals upregulation of gluconeogenesis in *mdh* cells.

605 Cells were grown in LB media without the addition of sugar. The only way to produce

606 pyruvate and glucose is through gluconeogenesis. A) Ion counts of malate levels in WT

607 and *mdh* cells. B) Ion counts of pyruvate levels in WT and *mdh* cells. C) Ion counts of

608 glucose-6P levels in WT and *mdh* cells. D) Ion counts of UD-NAG levels in WT and *mdh*

609 cells. Average of 3 independent experiments with standard deviation shown.

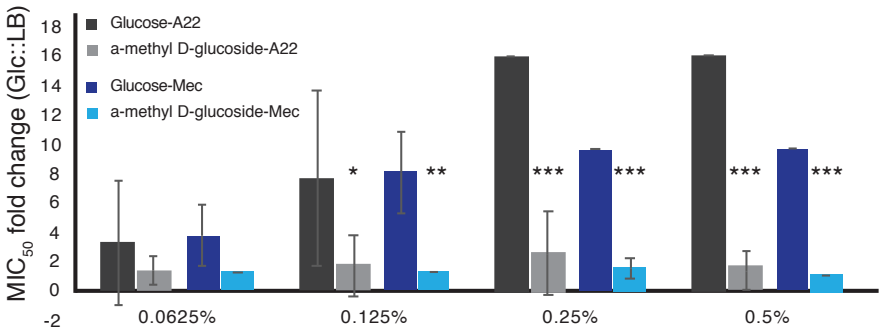

610

611 **Figure 3.** The addition of glucose to the media phenocopies the MIC phenotypes of the

612 *mdh* deletion. WT cells were grown in LB medium supplemented with the indicated

613 amount of either glucose or a non-hydrolizable glucose mimic, α-methyl D-glucoside (α

614 md). Cells were treated with either A22 (black bars) or mecillinam (blue bars). Error

615 shown in standard deviation from 3 independent experiments. * $p<.05$, ***$p<.001$

616 comparing glucose to α md for each condition.

617

618

619

620

621

622

623

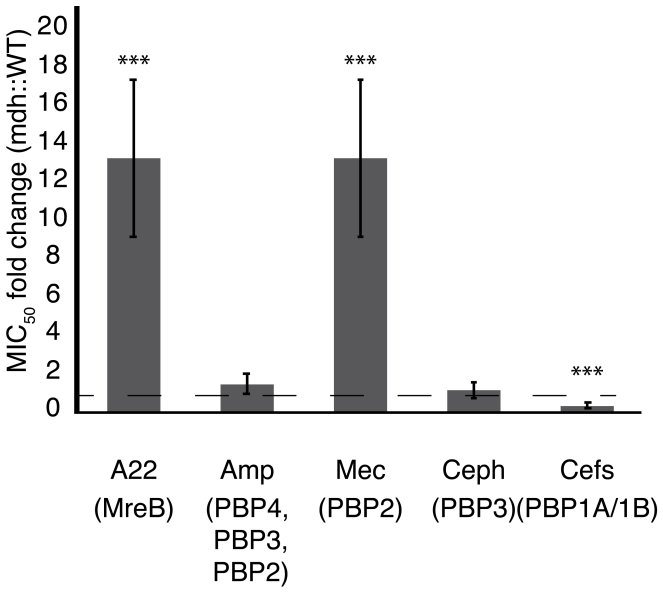

624

625 **Figure 4.** *mdh* mutation provides increased MIC specifically of A22 and mecillinam. MIC

626 assays were performed for the indicated antibiotics. A fold change of 1 (dotted line)

627 indicates no change. *** p>.001 comparing each strain to 1.

628

Category	**Count**
Metabolism	24
Genes of Unknown Function	14
Protein Activity	13
DNA Maintenance	12
Envelope	12
Transport	7
Gene Expression	4
Total	86

629 Table S1 Genes with high A_{22} MICs are enriched in metabolism. Gene ontology (GO) analysis of
630 the 86 strains displaying increased A_{22} MICs revealed a high concentration of genes focused in
631 metabolism.
632
633

Metabolism	Fold Change	Standard Deviation
fucO	12	4.62
gatZ	12	4.618802154
mdh	12	4.618802154
rsxA	12	4.618802154
bcsA	10.125	7.44283772
lipB	7	2
bioB	6.5	7.141428429
caiD	3.0125	3.44972825
hemE	2.75	3.5
purM	2.75	3.570714214
uxuB	2.3875	3.761731649
proB	2.375	3.772156766
purK	2.2625	3.830877837
hyfC	2.25	1.258305739
eutJ	2	0
garK	2	1.632993162
acs	1.7625	1.690845449
icd	1.5	0.577350269
rbsR	1.5	0.577350269
yodB	1.5	0.577350269
allB	1.3875	1.784364966
moeB	1.375	1.796988221

prpE	1.375	0.75
yjcS	1.375	0.75
Gene of Unknown Function	**Fold Change**	**Standard Deviation**
yedS	12	4.618802154
yeeN	10	7.659416862
yeeP	10	4
yjgZ	10	7.659416862
yrhA	4.375	4.190763654
ybaV	4.25	4.330127019
yobF	2.875	3.473110997
yfjR	2	0
yifN	1.75	1.658312395
glvG	1.625	1.600781059
yhcC	1.625	0.75
yhfK	1.625	0.75
yoeF	1.625	0.75
yjgX	1.375	1.75
Protein Activity	**Fold Change**	**Standard Deviation**
rpsT	10	4
rsuA	8	0
prfC	6.125	7.531876703
yihP	3.5	3

ykgM	3.5	3
tfaE	3.125	1.75
allR	2.625	3.591076904
uspG	2.5	3.674234614
ytfE	2.5	3.674234614
mtfA	2.375	3.75
fabR	2	1.632993162
napD	2	0
ibpB	1.5	1.683250823
DNA Maintenance	**Fold Change**	**Standard Deviation**
dnaT	12	4.618802154
hsdS	4	0
yjjB	3.5	1
caiT	2.5	3.674234614
dinF	2.5	3.674234614
rnhB	2.3875	3.761731649
aroP	2.375	3.75
priC	2.375	3.772156766
srmB	1.5	0.577350269
ttk (slmA)	1.5	0.577350269
torI	1.375	0.75
yrdD	1.375	0.75
Envelope	**Fold Change**	**Standard Deviation**

gmhB	10	4
clpP	9	5.033222957
wcaC	8.125	6.329494451
mltG	6.625	7.04006392
wcaK	6	4
bamB	3.125	3.326033674
ldtB	2.75	3.570714214
dtpA	2.25	3.840572874
oppC	1.75	1.658312395
mpl	1.625	1.600781059
ybbY	1.625	0.75
yeaY	1.5	1
Transport	**Fold Change**	**Standard Deviation**
wzzE	12	4.618802154
cls (clsA)	4.625	7.586995453
kdpF	2.75	3.5
kefG	2.375	3.772156766
mdtB	1.625	0.75
yhdY	1.625	0.75
ssuC	1.375	0.75
Gene Expression	**Fold Change**	**Standard Deviation**
narQ	12	4.618802154
yafT	8	0

yaeH	8	0
creC	1.5	1

634 Table S2. List of genes with screened for increased MIC_{A22}. Genes are sorted by ontology groups

635 and then listed in order of decreasing MIC_{A22}.

636

637

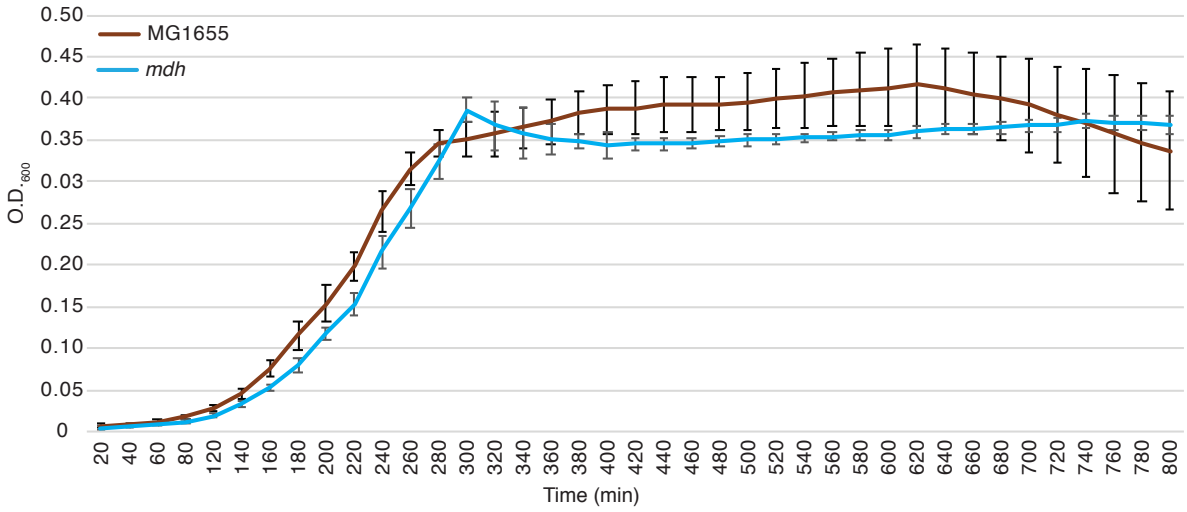

Figure 1S. *mdh* mutant grows the same as WT. WT and *mdh* cells were grown overnight in LB. Cells were equalized to the same $O.D._{600}$ and subcultured into fresh LB medium in a 96 well plate at a 1:100 dilution. The plate was grown at 37ºC with shaking in a Biotek Synergy plate reader. Error bars are standard deviation across wells in a plate. Data is a representative experiment.

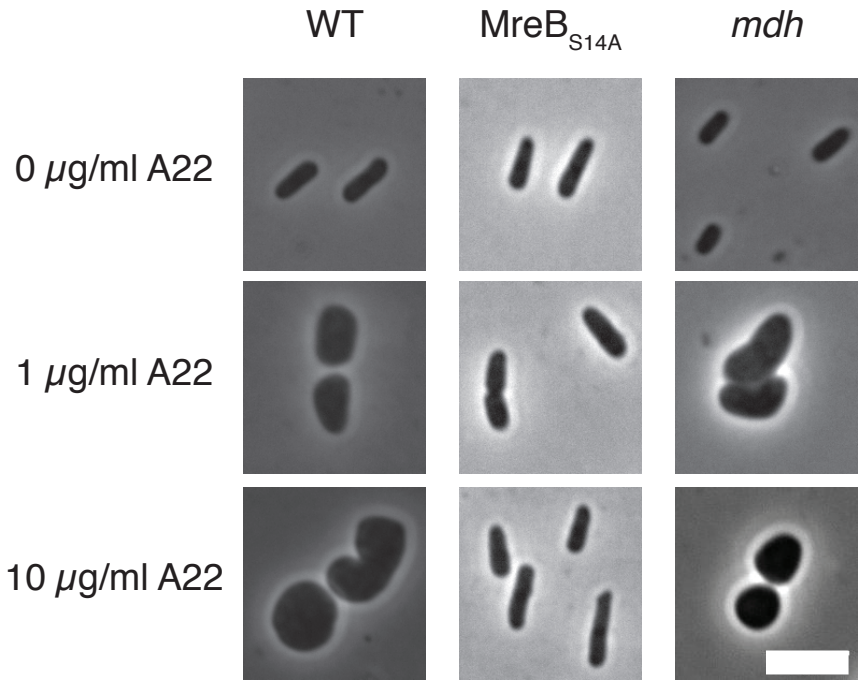

Figure 2S. *mdh* cells become round during A22 treatment. Cells were grown overnight and subcultured 1:1000 into fresh LB medium. Cells were grown for 4 hours in the 0 and 1 μg/ml A22. Cells were grown in LB for 2 hours before the addition of 10 μg/ml A22 for 2 hours. Images are representative of an experiment done in triplicate. Scale bar = 5 μm.

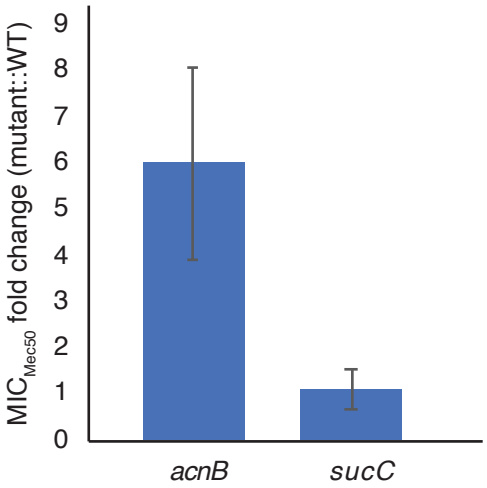

652

653 Figure 3S. *sucC* does not cause a change in mecillinam resistance. MIC_{mec} of *acnB* and

654 *sucC* mutants compared to WT type cells.

655